Economic Analysis of Integrated Renewable Energy System for Electrification of Remote Rural Area having Scattered Population

Alpesh M. Patel*‡, Sunil Kumar Singal**

*Research Scholar, AHEC, IIT Roorkee, Roorkee-247667, Uttarakhand, India

**Associate Professor, AHEC, IIT Roorkee, Roorkee-247667, Uttarakhand, India

(alpesh6815@gmail.com, sunilksingal@gmail.com)

‡ Corresponding Author; Alpesh M. Patel, 36, Azad Wing Hostel, IIT Roorkee campus, Roorkee-247667, Uttarakhand, India,

Tel: +91-9909983503, alpesh6815@gmail.com

Received: 14.07.2017 Accepted:13.08.2017

Abstract- The renewable energy sources (RES) are globally recognized as a suitable option for sustainable development in many off-grid applications. Recently, the integrated systems with two or more RES are being paid great attention for electrification of the isolated areas and found to be an acceptable solution rather than uneconomical grid extension. In the present study, the integrated renewable energy system (IRES) model is developed using solar, wind, biomass and biogas energy sources to meet the electricity demand of the isolated rural community of Khatisitara village of Gujarat state in India. The operational strategy for the IRES model is developed considering the distribution network losses as a system design parameter. The developed IRES model is optimized for minimum net present cost of the system using particle swarm optimization (PSO) algorithm in MATLAB environment. The well-established genetic algorithm (GA) was used to validate the results obtained from the PSO algorithm. Further, the effects of distribution losses (DL) on the system size, power reliability and economy have been evaluated. The sensitivity analysis was performed to assess the effect of economically influencing parameters on the developed model. Finally, the break-even analysis was performed for the grid extension distance to examine the economic feasibility of the IRES against grid extension. The simulation results show that the impacts of DL on the power reliability and economy of the IRES are significant. Further analysis shows that the IRES using locally available RES is a feasible option for rural electrification in the considered study area rather than grid extension.

Keywords Integrated renewable energy system, Off-grid system, Distribution loss, Economic feasibility, Grid extension.

1. Introduction

Electrical energy is the most useful form of energy which satisfies various needs of the human being. Presently, the fossil fuel based electricity generation is dominating the renewable energy (RE) source based power generation [1]. However, more use of fossil fuel is a matter of worry due to its dwindling nature and non-uniform distribution throughout the world. Also, enormous uses of such resources create a perilous situation such as global warming, acid rain, etc [2]. Presently, many regions around the world are facing flood and drought situation due to increasing use of fossil fuel based conventional energy sources [3].

Generally, urban areas are facilitated with various forms of energy but isolated rural areas of many developing countries are still struggling for electricity access to satisfy their daily needs. Electrifying such isolated areas can elevate the communities socio-economically [4]. The socio-economic and educational stirring of such communities can reduce the poverty level and contribute more in economic developement of the country [5]. The grid extension for electrification of the isolated hilly rural areas may be uneconomical due to poor load density and uneven terrain [6]. However, such areas are enriched with one or more renewable energy sources (RES) like solar, wind, small hydropower, biomass etc. These RES are environmentally benign, and it can effectively fulfill the energy demands of the community if developed and utilized properly [7].

An electrification of the remote area using single RE source may be inappropriate due to intermittent operating characteristics of the major RES [8]. In order to achieve the cost-effective and reliable solution, two or more available RES can be embedded together for power generation to fulfill the various energy needs of the remote community [9]. Generally, the integrated renewable energy system (IRES) is incorporated with energy storage devices to take care of the intermittent nature of RES [10–12]. For the off-grid IRES, the cost and power reliability play a vital role in success of such project [13]. However, the reliable systems are often costly and economic systems are usually less reliable, so to achieve the best trade-off between the cost and power reliability, different optimization techniques are used [14,15].

The integrated system using two or more energy sources has received much attention over last two decades for electrification of the remotely located areas. In past, many research studies have been conducted using various configurations of the IRES for a variety of off-grid applications. Mostly, the IRES configurations such as solar-wind [4,16,17], solar-wind-hydro [18], solar-wind-biomass [19], solar-biomass [20], solar-biogas [21] and solar-wind-biogas [22] have been presented in the past studies. Hybrid energy system model based on the combination of the renewable and conventional energy sources were also developed by many researchers to electrify rural areas [23,24].

Nandi and Ghosh [25] developed a hybrid energy system model for electrification of Kutubdia Island located on the Southern coast of Bangladesh using solar, wind and diesel based energy resources along with the battery. They performed a techno-economic analysis on different combination of the energy sources with 0% and 5% annual capacity shortage and determined an optimal combination of the resources having lowest net present cost and cost of energy. Rajanna and Saini [26] proposed an off-grid IRES model for rural electrification of un-electrified villages in Chamarajanagar district of Karnataka state in India. They investigated a feasibility of the system using different optimization power factor and expected energy not supplied (EENS). The developed model was optimized using genetic algorithm (GA) based approach. Xu et al. [27] presented the different implementation strategies for the rural electrification using microgrid approach. They discussed three different scenarios of electrification for the rural area in the Eastern Cape Province of South Africa. The different implementation strategies were compared based on the cost, performance, efficiency, equipment utilization factor and excess electricity generated. Upadhyay and Sharma [28] proposed an off-grid hybrid system model using solar, micro hydropower, biomass, biogas and diesel energy resources for electrification of the seven un-electrified villages in Dhauladevi block of Uttarakhand state, India. The developed model was optimized using GA, particle swarm optimization (PSO) algorithm and HOMER software. Dekker et al. [2] performed an economic analysis of solar and diesel source based hybrid energy system. They considered different climatic zones of South Africa for the analysis and optimal configurations of the system were obtained. Ismail et al. [29] developed an optimized model of the hybrid energy system using solar photovoltaic (SPV), micro-turbine, diesel generator and battery bank to electrify a small community in the Palestinian Territories. The developed model was optimized for minimizing the cost of energy using GA with the specified value of reliability index. They considered four types of photovoltaic (PV) panels, two types of mounting fixtures, four types of batteries and two types of micro-turbines in the analysis. Kanase-Patil et al. [30] proposed an integrated renewable energy optimization model using the micro hydropower generator, biomass generator (BMG), biogas generator (BGG), wind turbine generator (WTG) and SPV to satisfy the seasonally varying demand of the remote hilly area in India. They developed a correlation between the RE source size and their capital cost in order to suggest a suitable size of the RE system for the study area.

From the previously published works, it has been observed that the IRES based power generation schemes were proposed with different combinations of the resources to satisfy the energy demands of the community without considering the distribution network losses. The effect of the distribution loss (DL) on the power reliability, economy and size of the off-grid IRES has not yet been identified. In remote rural areas, the loads are generally scattered in nature [31], and the electrical distribution system, which connects various loads with the electrical generators, needs to be developed [32]. The electrical distribution system is the most critical component of the power system which affect the power reliability and cost of the electricity significantly [33]. For the off-grid IRES, the total power delivered to the end users can be calculated by subtracting the total power loss occurred in the distribution network from the total generated power [34]. The power losses are occurred naturally due to the irradiation and inevitable dissipation of the electrical energy in various equipment and conductors of the distribution system [35]. Distribution network losses account around 13% of total generated energy in developing countries. The higher distribution losses have a direct impact on the overall economy and efficiency of the system [36]. Further, it has been observed that the IRES model developed so far mainly consists of the solar and wind energy resources for the off-grid rural electrification; however, the IRES using solar, wind, biomass and biogas energy resources is found limited in the literature.

Based on the literature survey carried out, the present study deals with the modeling of IRES using the solar, wind, biomass and biogas energy sources along with the battery to meet the electricity demand of the isolated rural community having scattered population. The developed IRES model is optimized for the total net present cost minimization and combined techno-economic analysis have been carried out. The distribution loss has been considered as a design parameter, and the operational strategy is developed for the assessment of economic viability of the IRES model. Further, an attempt has been made to identify the impact of the DL on the power reliability, size and economy of the IRES. The sensitivity analysis has been performed by considering the variation in capital cost of the system components and the cost of feedstocks. Finally, the break-even analysis has been carried out for grid extension distance to identify the economic feasibility limit of the proposed IRES model against grid supply option. The statistical significance was analyzed by using MATLAB software.

2. Modeling Methodology

The IRES model is developed by considering the approach of modeling methodology as given in Ref. [4]. The brief discussion of the study area, demand estimation, and resource assessment are covered in this section.

2.1. Study area

In the present study, "Khatisitara", a small hamlet of Amirgadh taluka in Banaskantha district of Gujarat state, India has been considered as a study area. It is located about 10 km away from the state road and 8 km away from the last electricity distribution point. The study area is a semi-isolated, non-revenue small hamlet situated near the border of Gujarat and Rajasthan states in the hilly terrain, and the population belongs to the Dungri Garasia tribal community. The total population of the study area is 745, out of which 377 are male and 368 female. The location of the study area is shown in Fig. 1 [37–40].

2.2. Energy demand estimation

The total electrical energy demand of the study area is estimated based on the actual needs of the community. The total energy demand is divided into the different categories such as domestic, commercial, agriculture and community. The details such as appliances, their rating and sector wise quantities considered for demand estimation are given in Table 1.

The light emitting diode (LED) based lighting option is considered in the analysis due to its benefits over the compact fluorescent lamp and incandescent lamp [41]. The

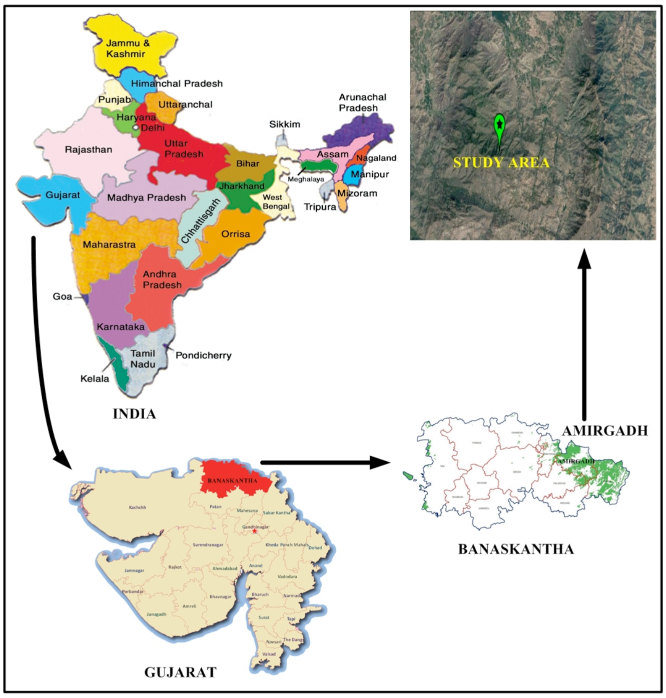

Fig. 1. Location of the study area [37–40]

energy demand estimation is carried out for the summer and winter seasons separately. The time span from March to October belongs to the summer season and November to February as winter season in the study area. The total daily energy demand of 347.881 kWh is estimated for the summer season with a peak value of 34.707 kWh, while the total daily energy demand of 210.766 kWh is estimated for the winter season with a peak value of 23.187 kWh. The daily energy demand profiles for the summer and winter seasons are shown in Fig. 2.

2.3. Resource estimation

The state of Gujarat is rich in terms of the availability of the RES such as solar, biogas, biomass, energy plantation, wind and tidal [42]. In order to estimate the potential of the locally available RE sources, an extensive survey was carried out in the study area and surrounding regions. The global solar radiation on a horizontal surface and wind speed data were obtained from the Indian Meteorological Department (IMD), Pune, India. The mean annual solar radiation on tilted surface is calculated as 4.40 kWh/m^2/day with a maximum value of 5.73 kWh/m^2/day in the month of May and a minimum value of 2.32 kWh/m^2/day in the month of November. The monthly average daily solar radiation and corresponding clearness index of the study area are given in Table 2.

The wind speed data provided by the IMD was recorded using an anemometer at 10-meter height. Then, the available wind speed data were extrapolated at 20 meter hub height using wind power-law equation given in equation (1) [43].

$$V_{hub} = V_{ane} \times \left(\frac{H_{hub}}{H_{ane}} \right)^{\alpha} \tag{1}$$

Where V_{hub}, V_{ane}, H_{hub}, H_{ane} and α are the wind speed at hub height, wind speed recorded by an anemometer, hub height of the WTG, height of an anemometer and the ground surface roughness (friction) coefficient respectively. In this study, α is taken as 0.2 [44].

The annually average wind speed is estimated at 5.26 m/s with a maximum value of 9.42 m/s in the month of May and a minimum value of 2.99 m/s in the month of November. The wind speed frequency distribution of the study area is shown in Fig. 3.

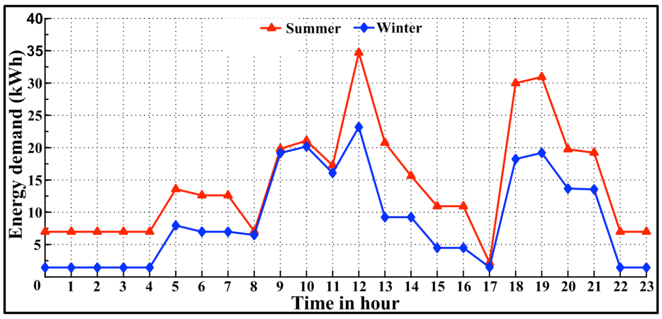

Fig. 2. Seasonal energy demand of study area

Table 1. Category and sector wise quantity of appliances

Sr. No.	Category and sector (with quantities) of load	Appliances	Rating in Watt	No. of points	Total quantities
1.	Domestic:				
	Households (123)	LED lamp	12	2 point	246
		Fan	45	2 point	246
		TV	70	1 point	123
2.	Commercial:				
	Shops (9)	LED lamp	12	1 point	9
		Fan	45	1 point	9
	Flour mill (1)	LED lamp	12	1 point	1
		Fan	45	1 point	1
		Motor	3750	1 point	1
3.	Agriculture:				
	Crop threshing machine (1)	Motor	5000	1 point	1
4.	Community:				
	Community hall (1)	LED lamp	12	3 point	3
		Fan	45	3 point	3
		Music system	500	1 point	1
	Dispensary (1)	LED lamp	12	4 point	4
		Fan	45	4 point	4
		Refrigerator	475	1 point	1
		Immersion rod	1000	1 point	1
	School (1)	LED lamp	12	10 point	10
		Fan	45	10 point	10
		Computer	150	1 point	1
		Music system	500	1 point	1
	Dairy (1)	LED lamp	12	3 point	3
		Fan	45	2 point	2
		Refrigerator	5000	1 point	1
	Water pumping system (1)	Motor	2238	4 point	4
	Street lights (40)	LED lamp	24	1 point	40

The study area has total 142.78 hectares of agriculture land, out of which 27.25 hectares are irrigated, along with the surrounding forest belt of approximately 157 hectares [45]. The wheat, maize and mustard are the dominating agriculture products of this area.

The total dry biomass potential from the forest foliage (fuelwood) and agriculture waste have been estimated as 9.42 tons/year and 56.72 tons/year respectively at 60 % collection efficiency. The total cattle strength has been estimated as 186 including 128 cows and 58 buffaloes. The total cattle dung availability has been estimated as 1290 kg/day at 60 % collection efficiency.

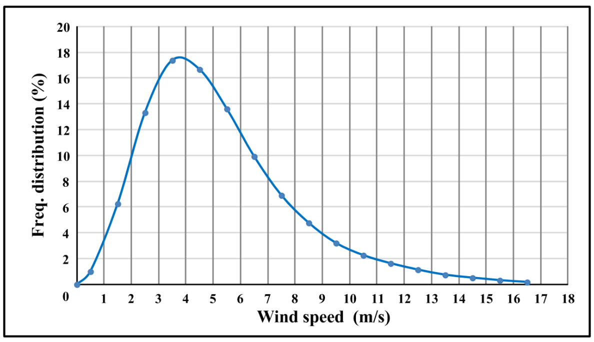

Fig. 3. Wind speed frequency distribution of study area

3. IRES Configuration

The integrated renewable energy system model has been configured by considering the solar, wind, biomass and biogas as energy sources for electricity generation and the battery bank as an energy storage element. In the present study, an attempt has been made to create a small autonomous microgrid which can satisfy the energy needs of the community. As the system consists of both AC and DC generating sources, the AC-DC hybrid configuration has been adopted. The proposed IRES configuration is shown in Fig. 4.

3.1. System component selection

In the present study, the RE technologies such as solar PV, WTG, BMG and BGG are considered for power generation to satisfy the electricity needs of the community. In this section, various system components used to formulate the IRES model and their specifications are discussed.

3.1.1. Solar energy system

In Gujarat state, Gujarat Energy Development Agency (GEDA) is the state nodal agency for promotion and

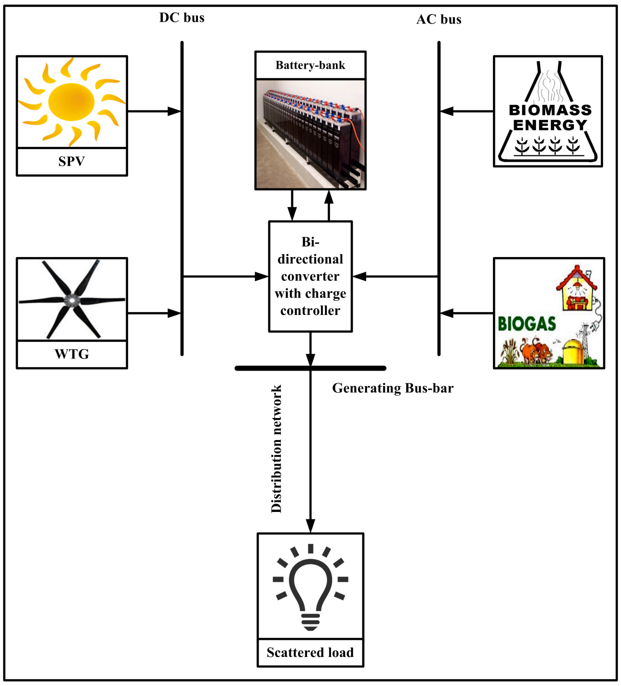

Fig. 4. Proposed IRES configuration

implementation of the alternative energy source based systems. The specifications of the solar PV module are obtained from the agencies empanelled by GEDA and given in Table 3 [46]. The annual operation and maintenance (O&M) cost of the SPV module is considered as 2.5 % of its capital cost, which is collectively taken as 0.7 INR/kWh based on its annual energy generation.

3.1.2. Wind energy system

From Fig. 3, it is seen that the study area has the highest frequency of 17.37 % for the wind speed between 3 to 4 m/s. So, the use of small rating WTG operating at low cut-in speed can extract more power from the wind. The specifications of the WTG system are obtained from the "Ministry of New and Renewable Energy", India empanelled agency [47] and given in Table 4. The annual O&M cost of the WTG is considered as 2.5 % of its capital cost which is collectively taken as 0.6 INR/kWh based on its annual energy generation.

Table 2. Monthly averaged daily solar radiation and clearness index of study area

Sr. No.	Month	Monthly average daily solar radiation (kWh/m^2/day)	Clearness index
1	January	4.54	0.53
2	February	4.70	0.51
3	March	5.72	0.58
4	April	5.29	0.52
5	May	5.73	0.57
6	June	4.88	0.49
7	July	3.40	0.33
8	August	4.14	0.41
9	September	2.73	0.28
10	October	4.77	0.51
11	November	2.32	0.29
12	December	4.57	0.54

Table 3. Specifications of SPV module

Parameter	Unit	Value
Rated (peak) power output (W_P)	watt	300
Open circuit voltage	volt	44.56
Maximum voltage	volt	38.88
Short circuit current	ampere	8.48
Maximum current	ampere	7.71
Module efficiency	%	15.5
Capital cost of SPV module	INR	10080
Installation cost of SPV module (@ 20% of capital cost)	INR	2016
Life of SPV module	year	20

3.1.3. Biomass generator system

The biomass gasification system along with the gas operated engine-generator set is considered for electricity generation. The economic assessment of the BMG system has been carried out by considering the capital cost, O&M cost and fuel (biomass) cost. The capital cost of BMG system includes the cost of gasifier, gas handling unit, engine-generator set, accessories and civil works. The cost of civil works includes the cost of foundation, storage premise for raw fuel (biomass) and storage tank for the producer gas. The fuel preparation (chopping, drying, etc) and handling expenses are incorporated in the overall O&M cost of the BMG system. The annual O&M cost of the whole unit along with auxiliary equipment is taken as 10% of the total cost of the gasifier and engine-generator set, which is collectively taken as 1.27 INR/kWh based on the annual energy generated by the BMG unit. Based on the estimated biomass potential, 15kW$_e$ BMG system is considered in the analysis. The specifications of BMG system are given in Table 5 [48].

3.1.4. Biogas generator system

Biogas to electricity generation involves two stage process: 1) The biogas is produced from the raw fuel (cattle dung) through an anaerobic digestion, and 2) The electricity is produced from the biogas using gas engine-generator set. The economic assessment of the BGG system has been carried by considering the capital, O&M and fuel costs.

Table 4. Specifications of WTG

Parameter	Unit	Value
Rated power	kW	3.3
Cut-in wind speed	m/s	2.7
Cut-out wind speed	m/s	20
Rated wind speed	m/s	10.5
Swept area of wind turbine	m^2	16.4
Efficiency of WTG system	%	90
Power coefficient of WTG system	---	0.46
Capital cost of WTG system	INR	210000
Installation cost of WTG system (@ 30% of capital cost)	INR	63000
Life of WTG system	year	20

Table 5. Specifications of BMG system

Parameter	Unit	Value
Capital cost of gasifier system	INR	352500
Capital cost of engine-generator set	INR	412500
Capital cost of civil works	INR	125000
Conversion efficiency	%	20
Cost of biomass	INR/kg	2.00
Specific consumption of biomass	Kg/kWh	1.5
Life of civil works	year	25
Life of gasifier system	hour	10000
Life of engine-generator set	hour	15000

Table 6. Specifications of BGG system

Parameter	Unit	Value
Capital cost of civil works	INR	228445
Capital cost of engine-generator set	INR	300000
Annual operation and maintenance cost of system	INR/kWh	1.3
Conversion efficiency	%	27
Cost of cattle dung	INR/kg	0.20
Specific consumption of biogas	m^3/kWh	0.5
Quantity of dung required to produce 1 m^3 biogas	Kg/m^3	25
Life of civil works	Year	25
Life of engine-generator set	hour	20000

The capital cost of the BGG system is estimated by considering the cost of the civil works and engine-generator set with accessories. The cost of civil works includes the cost of digester, inlet (mixing) tank, outlet (overflow) tank and other accessories, foundation cost of engine-generator set and storage tank cost for the biogas. The cost of civil works is estimated using the item rates, which are published in "Schedule of Rates" by the Government of Gujarat for the FY 2016-17. The raw fuel and product biogas handling expenses are incorporated in the overall O&M cost of the BGG system. The annual O&M cost of the whole unit is estimated at 8% of the cost of engine-generator set and 2% of the cost of civil works, which are collectively taken as 1.3 INR/kWh based on the annual energy generated by the BGG system. Based on the availability of cattle dung in the study area, the biogas plant of 45 m^3 and engine-generator set of 10 kW_e are considered in the analysis. The specifications of the BGG system are given in Table 6 [48].

3.1.5. Battery and bi-directional converter with charge controller

The specifications of the battery and bi-directional converter with charge controller (BDC-CC) used in the analysis are given in Table 7 [49,50].

4. Mathematical Modeling of IRES Components

In order to evaluate performance of the system, the mathematical modeling of the IRES components has been carried out and discussed in this section.

4.1. SPV system

The hourly power output (in kW) from the SPV panel array can be calculated by using equation (2) [51].

$$P_{PV} = P_{RAT,STC} \times F_{DR} \times \left(\frac{H_t}{H_{t,STC}} \right) \times N_{PV} \quad (2)$$

Where $P_{RAT,STC}$ is the rated power of selected SPV module under standard test conditions, F_{DR} and N_{PV} are the number and derating factor of the SPV module, H_t is an hourly solar radiation incident on the SPV module, $H_{t,STC}$ is solar radiation at standard test condition.

4.2. Wind turbine generator

At any hour t, the power output (in kW) from the WTG system can be calculated by using equation (3) [52].

$$P_{WTG}(t) = \begin{cases} 0, & \text{if } V_h < V_{CI} \& V_h > V_{CO} \\ \left[\dfrac{0.5 \times C_P \times \rho_{air} \times \eta_W \times A_{WT} \times N_{WT} \times (V_h(t))^3}{1000} \right], & \text{if } V_{CI} \le V_h < V_R \\ P_R, & \text{if } V_R \le V_h \le V_{CO} \end{cases} \quad (3)$$

Where P_R is the rated power of the WTG, C_P is a power coefficient of the WTG, ρ_{air} is the air density, η_W is an efficiency of the WTG, A_{WT} is the swept area of the rotor, N_{WT} is a number of WTG and V_h is an hourly wind speed. The symbols V_R, V_{CI} and V_{CO} represent the rated, cut-in and cut-out wind speed of the selected WTG respectively.

4.3. Biomass generator

Total biomass potential of the study area is estimated as 66.14 tons/year. The operating hours of the BMG system are considered as 11 hours per day. The hourly power output (in kW) from the BMG system can be determined by using equation (4) [53].

$$P_{BMG} = \frac{Q_{BM} \times CFV_{BM} \times \eta_{BMG} \times 1000}{OH_{BMG} \times 365 \times 860} \quad (4)$$

Where Q_{BM}, and CFV_{BM} are the quanity (ton/year) and calorific value (kcal/kg) of the biomass respectively; η_{BMG} and OH_{BMG} indicate the total conversion efficiency and daily operating hours of the BMG system respectively. The calorific value represents the release of energy content from the fuel when burnt in the air and can be indicated by the higher and lower heating values. The lower heating value of the fuel is a proper value for subsequent use [54]. The power output from the BMG is calculated by considering the quantities and lower heating value of each type of biomass.

Table 7. Specifications of battery and BDC-CC

Parameter	Unit	Value
Lead acid battery:		
Rated capacity	Ah	100
Rated voltage	volt	12
Depth of discharge	%	80
Charging efficiency	%	90
Discharging efficiency	%	100
Hourly self-discharge rate	%	0.02
Capital cost of unit	INR	9300
Annual O&M cost of unit (@ 3% of capital cost)	INR	279
Lifespan	year	3
Bi-directional converter with charge controller:		
Rated capacity	kW	25
Converter efficiency	%	95
Charge controller efficiency	%	90
Capital cost of unit	INR	175000
Annual O&M cost of unit (@ 3% of capital cost)	INR	5250
Lifespan	year	10

The calorific value of biomass such as wheat straw, maize stalks, mustard stalks and fuel wood are taken as 17.15 MJ/kg (4098.94 kcal/kg), 16.67 MJ/kg (3984.22 kcal/kg), 17 MJ/kg (4063.10 kcal/kg) and 4015 kcal/kg respectively [55,56].

4.4. Biogas generator

The biogas potential has been estimated based on the daily availability of the cattle dung. The dung production has been considered as 10 kg/day for cow and 15 kg/day for buffalo. It has been assumed that 0.036 m^3 of biogas is produced from one kg of cattle dung [56]. The total biogas production is estimated as 46.44 m^3/day and considered for power generation. The operating hours of the BGG are considered as 6 hours per day. The hourly power output (in kW) of the BGG can be determined by using equation (5) [28].

$$P_{BGG} = \frac{Q_{BG} \times CFV_{BG} \times \eta_{BGG}}{OH_{BGG} \times 860} \tag{5}$$

Where Q_{BG}, CFV_{BG}, η_{BGG} and OH_{BGG} are the quanty of biogas (m^3/day), calorific value of the biogas (4700 kcal/m^3) [56], total conversion efficiency of the BGG and daily operating hours of the BGG system respectively.

4.5. Battery

The storage batteries are an unavoidable component of the off-grid IRES due to the stochastic nature of major RES [57]. At any hour t, the state of charge (SOC) of the battery can be calculated by using the parameters such as energy available on generating bus-bar at hour t, energy demand at hour t, battery self-discharging rate and previous hour SOC of the battery. During charging, the SOC of battery bank can be calculated by using equation (6) [58].

$$SOC(t+1) = \left(SOC(t) \times (1-\sigma)\right) + \left(\left(E_{gen,T}(t) - E_D(t)\right) \times \eta_{ch} \times \eta_{rec}\right) \tag{6}$$

Where σ, $E_{gen,T}(t)$, $E_D(t)$, η_{ch} and η_{rec} indicate the houly self-discharging rate of the battery, total energy available on generating bus-bar at hour t, energy demand at hour t, charging efficiency of the battery and rectification efficiency of the converter respectively.

During discharging cycle of the battery, the SOC can be calculated by using equation (7).

$$SOC(t+1) = \left(SOC(t) \times (1-\sigma)\right) - \left[\frac{E_D(t) - E_{gen,T}(t)}{\eta_{dch} \times \eta_{inv}}\right] \tag{7}$$

Where η_{dch} and η_{inv} represent the discharging efficiency of the battery and inverter efficiency respectively.

5. Problem Formulation

This section presents the formulation of the objective function, system design constraints and system design parameter.

5.1. Objective function

In order to evaluate the economic viability of the system, minimization of total net present cost (TNPC) is taken as an objective function. The objective function of the proposed study is given by equation (8).

$$\text{Minimize: } TNPC = \frac{C_{TA}}{F_{CR}} \tag{8}$$

Where C_{TA} and F_{CR} indicate the total annualized cost of the system and capital recovery factor respectively.

The capital recovery factor re-builds the present value of different system cost into the stream of equal annual cost over the project life span. The capital recovery factor can be calculated, using equation (9) and (10) [4,9].

$$F_{CR} = \frac{i_r(1+i_r)^{n_p}}{(1+i_r)^{n_p} - 1} \tag{9}$$

$$i_r = \frac{i_{nom} - i_{inf}}{1 + i_{inf}} \tag{10}$$

Where i_r, n_p, i_{nom} and i_{inf} represent the annual real interest rate, project life span, nominal annual interest rate and annual inflation rate respectively.

The total annualized cost of the system is calculated by considering the annualized capital investment cost, annualized O&M cost and annualized fuel cost of all system components using equation (11) [49].

$$C_{TA} = C_{AC} + C_{AOM} + C_{AF} \tag{11}$$

Where C_{AC}, C_{AOM} and C_{AF} represent the annualized capital cost, annualized O&M cost and annualized fuel cost respectively for all system components.

The annualized capital cost of the system is the sum of the annualized capital cost of all system components such as PV panel, WTG, BMG, BGG, battery and BDC-CC, and it can be calculated by using equation (12).

$$C_{AC} = \sum_{m=1}^{6} \left(C_{C,m} \times F_{CR,m} \right) \quad (12)$$

Where $C_{C,m}$ and $F_{CR,m}$ indicate the capital cost and capital recovery factor for m^{th} component of the system respectively.

Further, the annualized operation and maintenance cost of the system is the sum of annualized operation and maintenance cost of all system components. It can be calculated by using equation (13) [59].

$$C_{AOM} = \left\{ \sum_{t=1}^{8760} \sum_{i=1}^{4} \left(C_{OM,i} \times E_{gen,i}(t) \right) + \left(C_{OM,B} + C_{OM,BDC\text{-}CC} \right) \right\} \quad (13)$$

Where $C_{OM,i}$, $E_{gen,i}(t)$, $C_{OM,B}$ and $C_{OM,BDC\text{-}CC}$ indicate the O&M cost of i^{th} resource, energy generated by i^{th} resource at t^{th} hour, annual O&M cost of the battery and the annual O&M cost of the BDC-CC respectively.

In the present study, the BMG and BGG feedstocks are considered as fuel. The annualized fuel cost of the system is calculated by using equation (14) [49].

$$C_{AF} = \left\{ \begin{array}{l} \left(P_{BMG} \times SC_{BM} \times CUF_{BMG} \times C_{BM} \right) + \\ \left(P_{BGG} \times SC_{BG} \times CUF_{BGG} \times C_D \times Q_D \right) \end{array} \right\} \times 8760 \quad (14)$$

Where SC_{BM}, CUF_{BMG} and C_{BM} represent the specific consumption of biomass, capacity utilization factor of BMG and cost of the biomass respectively. SC_{BG}, CUF_{BGG}, C_D and Q_D indicate the specific consumption of biogas, capacity utilization factor of BGG, cost of the dung and the quantity of dung required to generate 1 m^3 of biogas respectively.

Finally, the levelized energy cost (LEC) has been calculated, using equation (15).

$$LEC = \frac{C_{TA}}{E_{TG}} \quad (15)$$

Where E_{TG} is the annual generated energy served.

5.2. System design constraints

In order to operate the system within pre-specified range of different parameters, the system design constraints are used in the simulation. The IRES model is optimized with following design constraints.

5.2.1. Reliability constraint

It is often practical to investigate the system reliability during the optimization process. The energy index of reliability (EIR) is widely used to evaluate the power reliability of the off-grid system [60,61]. The EIR, to evaluate IRES reliability, can be calculated by using equation (16) to (18).

$$EIR = \frac{E_{AS}}{E_{TD}} \quad (16)$$

$$E_{AS} = E_{TD} - EENS \quad (17)$$

$$EENS = \sum_{i=1}^{8760} E_{Di} \quad (18)$$

Where E_{AS}, E_{TD}, EENS and E_{Di} represent the actual annual energy served, annual energy demand, expected energy not served and an hourly energy demand not served at i^{th} hour respectively.

5.2.2. Operating limit constraint of battery bank

The overcharging and over-discharging of the battery drastically reduce its life. In order to prevent the overcharging and over-discharging of the battery, its operating limit constraints have been used in the simulations. At any hour t, the capacity of the battery bank (E_{BATT}) should lie between its maximum and minimum operating capacity. The related constraints used in the simulations are given by equation (19) to (21).

$$E_{Bmin} \le E_{BATT}(t) \le E_{Bmax} \quad (19)$$

$$E_{Bmin} = \left(\frac{V_B \times S_B \times N_{BATT}}{1000} \right) \times SOC_{min} \quad (20)$$

$$E_{Bmax} = \left(\frac{V_B \times S_B \times N_{BATT}}{1000} \right) \times SOC_{max} \quad (21)$$

Where E_{Bmin}, E_{Bmax}, V_B, S_B, N_{BATT}, SOC_{min} and SOC_{max} represent the minimum operating capacity of the battery bank, maximum operating capacity of the battery bank, rated voltage of each battery, rated capacity of each battery (in Ah), number of battery, minimum SOC value of the battery and maximum SOC value of the battery respectively.

At each hour, the total energy generated is compared with the total energy demand and difference is evaluated in the algorithm. The surplus energy available can be used for battery charging provided the SOC of the battery is below its maximum limit. Further, the stored energy of the battery can be used during the time when the demand exceeds the total generation provided the SOC of the battery is above its minimum level.

5.3. System design parameter

In the present study, the distribution loss has been considered as system design parameter to measure its accountability in the system component sizing, system reliability and system economy. The actual DL data of the concerned distribution company for the study area have been used in the analysis. The study area belongs to the operating region of the Uttar Gujarat Vij Company Limited (UGVCL). The DL data of the UGVCL network are given in Table 8 [62]. The data from FY 2005-06 to FY 2015-16, given in Table 8, represent the actual distribution loss occurred in the UGVCL network; however, the DL value for FY 2016-17 indicates the projected distribution loss of the network. The analysis have been carried out for the DL value of 1 to 15%; however, the different results are interpreted at 10 % distribution losses.

6. Optimization

The unit size optimization of the multi-source integrated system is often more complicated due to the involvement of a large number of the variables and parameters [63]. The heuristic search based algorithms are suitable tools for solving the complex problems of optimization. It can effectively handle the stochastic nature of the variables and easily escape from the local optima in search space [64]. Among heuristic techniques, the PSO developed by Kennedy and Eberhart [65] is one of the most popular algorithm due to its simplicity, good efficiency and fast convergence. PSO is a reliable meta-heuristic optimization technique, which reaches to the global optimum solution without using expensive computational operations [66]. Thus, the developed IRES model is optimized using PSO technique in MATLAB environment. Initially, the optimal net present cost and levelized energy cost of the proposed IRES have been evaluated without considering the distribution network losses and then further optimized by considering the distribution losses. During the optimization process, a care has been taken to maintain the system reliability. The implementation procedure of PSO algorithm for the formulated problem is explained through flow chart shown in Fig. 5.

The optimal results obtained using the PSO algorithm are validated by using the well-established genetic algorithm optimization technique. Genetic algorithm is a powerful tool for obtaining the optimal sizing of the integrated system components [67–70]. GA is a population-based artificial intelligence technique, which performs the computations using selection, crossover and mutation operators to obtain the optimal solution [26]. The steps invloved in GA for the formulated problem are depicted by the flowchart shown in Fig. 6. The results obtained using PSO and GA algorithm are discussed in Section 7.

6.1. Operational strategy

In order to find the optimal sizing of IRES components, the operational strategy has been developed by considering the various factors such as energy balance between total generation and total demand, operating limits of different energy sources, seasonally variable loads, required battery capacity, system reliability, excess energy (EE) generated and distribution losses.

Table 8. Distribution losses of UGVCL network

Sr. No.	Finance year	Distribution loss (%)
1	2005-06	19.45
2	2006-07	15.82
3	2007-08	17.35
4	2008-09	14.57
5	2009-10	17.36
6	2010-11	06.61
7	2011-12	09.81
8	2012-13	14.50
9	2013-14	06.54
10	2014-15	09.20
11	2015-16	11.07
12	2016-17	10.00 (projected)

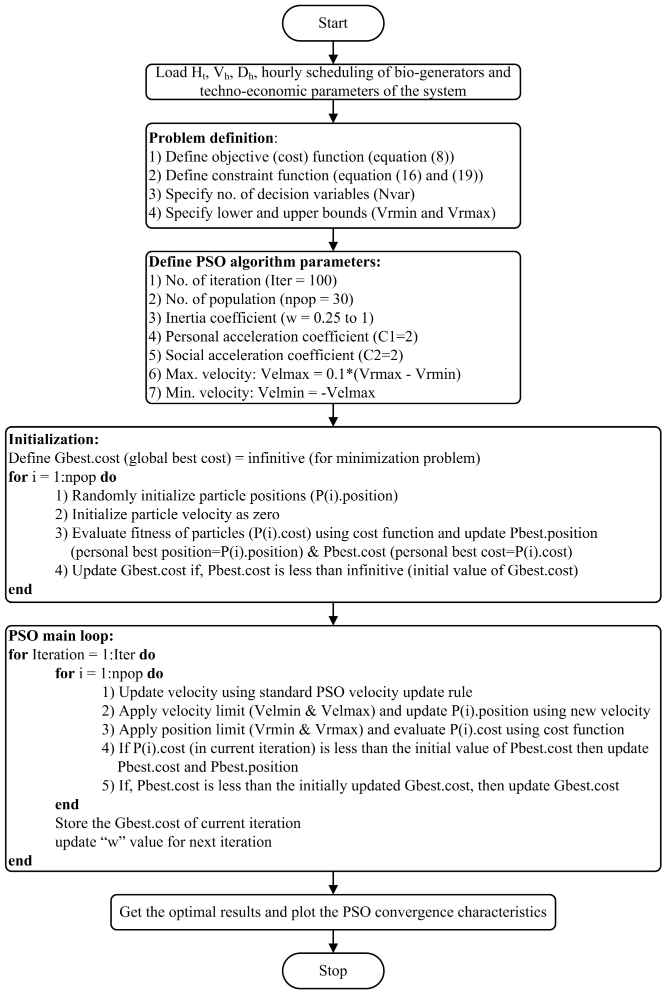

Fig. 5. Flowchart of PSO algorithm

In the present study, SPV, WTG and bioenergy generators are considered for the power generation. The solar and wind energy resources are stochastic in nature. Biomass and biogas, being more predictable energy resources, are useful during the peak hours. The priority of operation has been given to the bioenergy resources till its full exhaustion. From the energy demand profile of the study area, it is observed that the consumption is more during 9^{th} to the 14^{th} and 18^{th} to 21^{st} hours in a day. If the operation of bioenergy generators is scheduled during these hours, it will be easy to satisfy the peak hour demands. Based on the estimated potential of the bioenergy resources, the BMG of 15 kW_e and BGG of 10 kW_e are considered in the analysis which can operate for 11 hours and 6 hours respectively in a day. The operating schedule of BMG and BGG are shown in Fig. 7.

The steps for operational strategy of developed IRES model are discussed below.

- ➢ The hourly solar radiation, hourly wind speed, hourly energy demand (D_h), hourly output of bio-generators, system design constraints and techno-economic specification

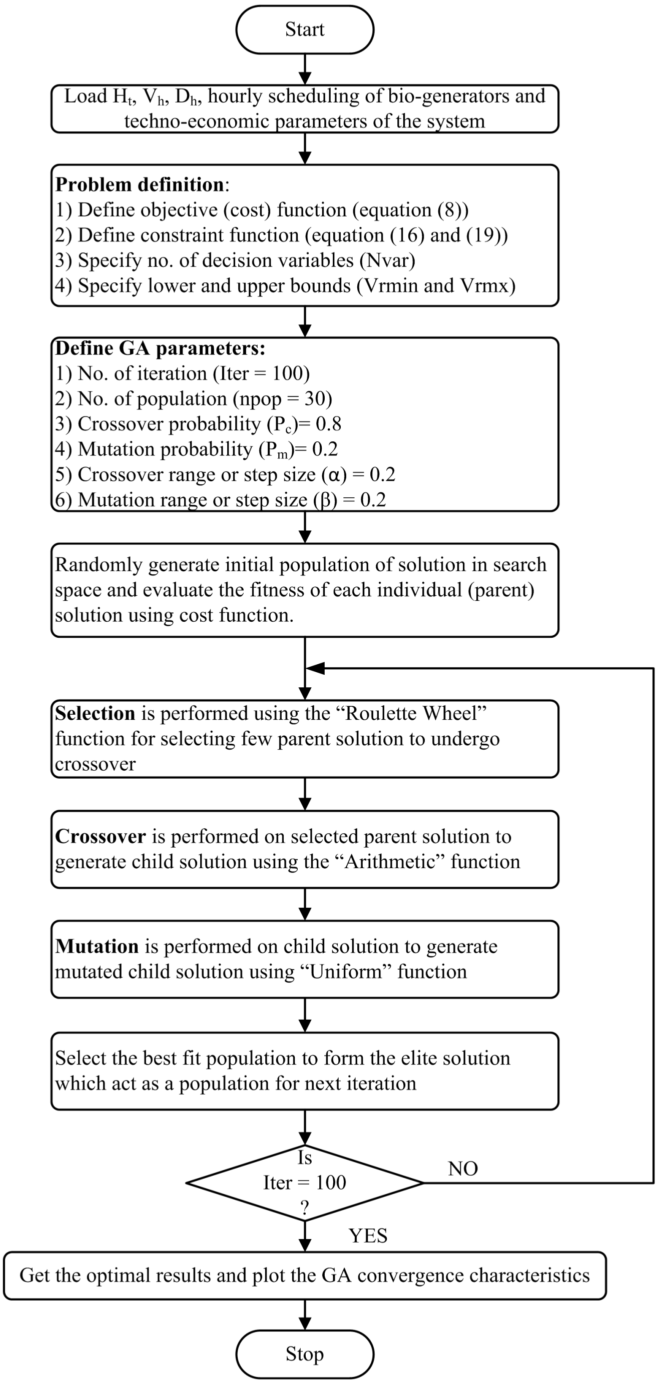

Fig. 6. Flowchart of GA algorithm

of IRES components have been considered as simulation input in the algorithm.

- At each simulation, the total energy available on generating bus-bar is compared with the total energy demand and the optimal solution is obtained from the set of decision variables where $E_{gen,T}$ is greater than or equal to E_{TD}.
- The distribution loss of the network is estimated and the corresponding power reliability of the system is evaluated for the optimal IRES configuration.
- Further, an optimal configuration of the IRES is again obtained to compensate the distribution losses and corresponding values of the $E_{gen,T}$, TNPC, LEC, EE, N_{PV}, N_{WT} and N_{BATT} are evaluated.
- The economic oversize factor (EOSF) for the optimal IRES at each DL has been evaluated with respect to the DL free optimal IRES based on the comparison of TNPC.
- The sensitivity analysis has been performed to measure the effect of the economically influencing parameters on behavior of the IRES.
- Finally, the economic feasibility of the developed IRES model has been examined by conducting the break-even analysis for the grid extension distance.

The flowchart for the operational strategy of proposed IRES is shown in Fig. 8.

7. Results and Discussion

Following the operational strategy as discussed in Section 6.1, the simulation results are obtained for the various parameters considered under the present study. The life span of the project, annual nominal interest rate and annual inflation rate have been considered as 20 years, 10% and 6% [71] respectively. The optimal results have been obtained in terms of the net present cost and levelized cost of the system. In order to have a reliable system, the EIR value has been set equal to unity in each simulation. The simulation results are divided into following two sub-sections.

7.1. Simulation results without considering distribution loss

The optimal configuration of the IRES has been obtained without considering the distribution losses for 0% annual energy shortage at the user end using GA and PSO algorithm in the MATLAB environment. The optimal results obtained using GA and PSO algorithm are given in Table 9.

For the proposed optimization problem, the optimal solution found at 33rd iteration in GA, while the PSO reached an optimal solution at 29th iteration. The total computational time for the annual analysis have been observed as 3.58 and 5.11 seconds for the PSO and GA respectively by using the Intel Core i5, 3.3 GHz processor with 8 GB memory (RAM) based computer system. The iterative convergence curve of the GA and PSO algorithm for the total net present cost of the system is shown in Fig. 9.

In comparison with GA, more efficient and superior convergence has been achieved by using the PSO algorithm, hence further discussion has been made based on the results obtained using PSO algorithm. The optimal configuration of the proposed IRES consists of two WTG of 3.3 kW, 53 SPV modules of 300 W_P, one biomass generator of 15 kW_e, one

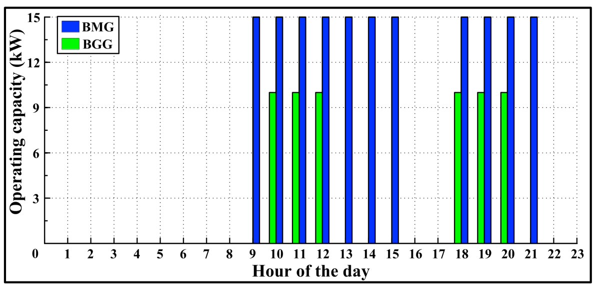

Fig. 7. Operating schedule of BMG and BGG

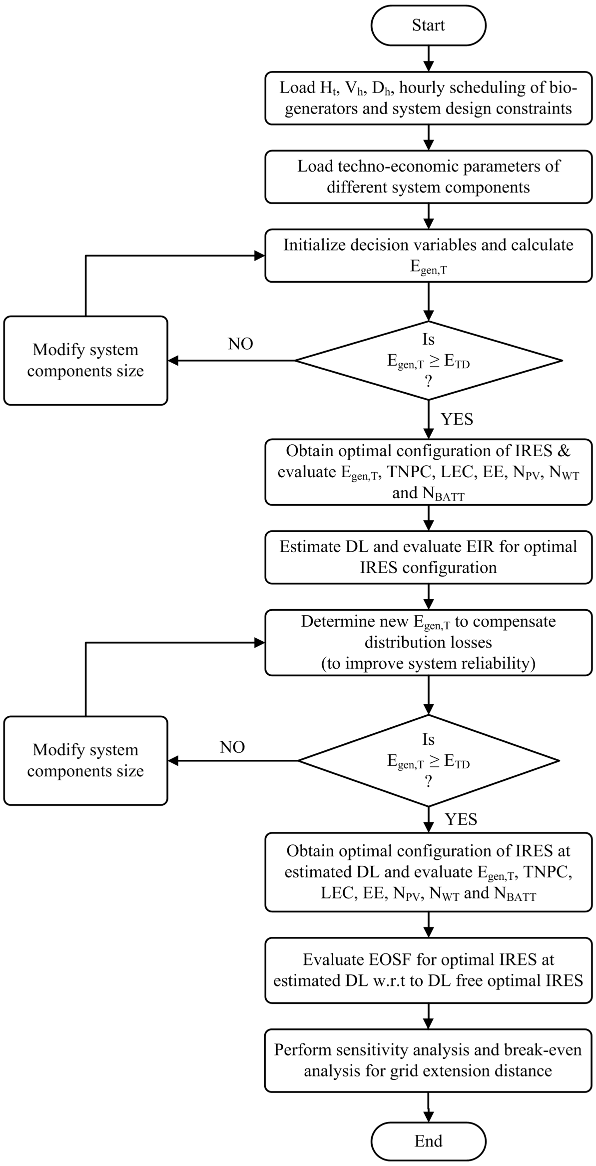

Fig. 8. Operational strategy of proposed IRES

biogas generator of 10 kW_e and 45 batteries of 100 Ah to meet the estimated electricity demand. The total annualized cost, total net present cost and levelized energy cost of the optimal system configuration have been obtained as INR 859152.74, INR 13421752.84 and INR 7.77 per unit of electricity respectively. For the optimal IRES configuration, 5246.26 (4.74%) kWh excess energy is generated annually. Fig. 10 shows the monthly averaged electrical energy generated by different RES for an optimal system. From Fig. 10, it is found that the BMG contribute maximum in the annual energy generation followed by the BGG, SPV and WTG. The breakdown of the total net present cost for the optimal IRES configuration is shown in Fig. 11. From Fig. 11, it has been observed that the BMG (48.76 %) contribute maximum in TNPC of the optimal IRES followed by the battery (20.02%), BGG (15.50%), SPV (7.79%), WTG (4.91%) and BDC-CC (3.02 %).

Table 9. Optimal results obtained using GA and PSO algorithm

Sr. No.	Optimal results	Optimization technique	
		GA	PSO
1	System components	2 WTG, 72 SPV module, 49 battery, 1 BMG, 1 BGG	2 WTG, 53 SPV module, 45 battery, 1 BMG, 1 BGG
2	TAC (INR)	893204.55	859152.74
3	TNPC (INR)	13953712.81	13421752.84
4	LEC (INR/kWh)	8.08	7.77
5	EE (kWh)	12131.05	5246.26
6	No. of iteration	33	29
7	Computational time (second)	5.11	3.58

7.2. Simulation results considering distribution losses

The distribution loss values of 1 to 15% have been used in the simulations and the results are obtained. However, the results are interpreted at 10% DL. The optimal configuration of the IRES has been obtained at each DL for 0% annual energy shortage at the user end.

7.2.1. *Effect on system reliability*

In order to evaluate the effect of DL on IRES reliability, the optimal configuration of the IRES as obtained in Section 7.1 is further considered for the analysis. The EIR of the system is evaluated at each DL loss value. The variation in EIR for different values of the DL is shown in Fig. 12. It is found that the system reliability is decreasing with the rise in DL. The result shows that the system reliability gets deteriorated, if the DL is not considered in the IRES design. From Fig. 12, it is observed that the EIR value is more than 1 (indicated by red arrow) for DL up to 4.52%. This is due to the presence of the excess energy in the system. However, from 4.53% onwards the EIR value starts reducing. At 10% distribution loss, the EIR value has been evaluated as 0.9427 (94.27%). It shows that the reliability of the off-grid IRES would be compromised by 5.73% if it is designed without considering distribution losses of 10%. The results

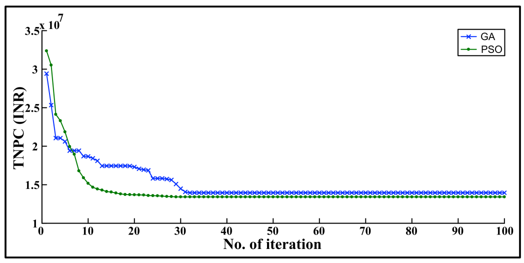

Fig. 9. Convergence curve of GA & PSO for TNPC of IRES

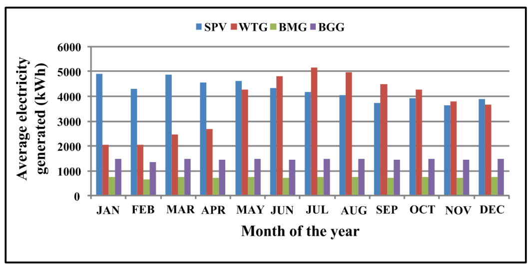

Fig. 10. Monthly averaged energy generated by RES

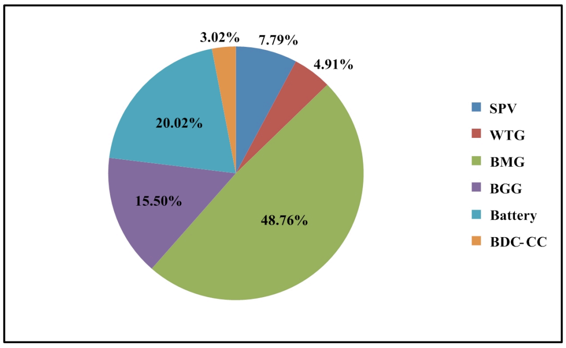

Fig. 11. Breakdown of TNPC for the optimal IRES Configuration

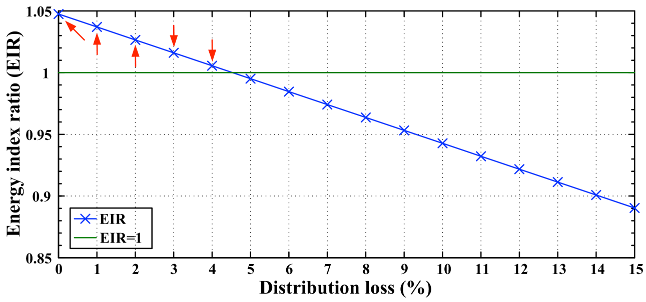

Fig. 12. Effect of DL on IRES reliability

demonstrate that the distribution losses are significantly affecting IRES reliability, if not considered in the design.

7.2.2. Effect on system component size

As discussed in Section 7.2.1, the distribution losses are significantly affecting the system reliability. In order to maintain power reliability of the off-grid IRES, the size of the IRES component needs to be revised accordingly. In order to evaluate the effect of the DL on the IRES component size, the optimal configuration of the IRES is obtained at each distribution loss value with 0% annual energy shortage at the user end. The number of SPV modules, WTG and battery for the optimal configuration of the IRES at each DL value are given in Table 10. The size and operating schedule of the BMG and BGG are kept fixed, hence their details are not included in Table 10. The optimal configuration of the IRES at 10% DL consists of three WTG of 3.3 kW, 73 SPV modules of 300 W_P, biomass generator of 15 kW_e, biogas generator of 10 kW_e and 53 batteries of 100 Ah to meet the estimated electricity demand. The results show that the IRES component size is considerably changed to compensate the distribution losses. In order to compensate 10% DL, the additional 20 SPV modules, 1 WTG and 8 batteries are required to satisfy the estimated energy demands compared to DL free optimal IRES.

7.2.3. Effect on system economy

In order to compensate the distribution losses, the size of IRES components is growing considerably, which will increase the overall cost of the IRES. Here, the economic increment of the optimal IRES corresponding to DL loss is represented by an economic oversized factor. The EOSF has been evaluated by taking the ratio of the TNPC of the

Table 10. Effect of DL on IRES component size

Distribution loss (%)	No. of SPV module	No. of WTG	No. of battery
0	53	2	45
1	36	3	44
2	59	2	46
3	44	3	46
4	67	2	48
5	90	1	5
6	74	2	50
7	78	2	51
8	83	2	52
9	69	3	52
10	73	3	53
11	94	2	54
12	78	3	54
13	121	1	58
14	109	2	58
15	94	3	58

optimal IRES at DL loss and the TNPC of the DL free optimal IRES. The TNPC and LEC of the optimal IRES at each DL value are determined and shown in Fig. 13. The TNPC and LEC of the optimal IRES at 10% DL are obtained as INR 14537289.65 and 8.42 INR/kWh respectively. The EOSF for the optimal configuration of IRES at each DL value along with the excess energy generated is shown in Fig. 14. For the optimal IRES at 10% DL, the TNPC and corresponding EOSF have been evaluated as INR 14537289.65 and 8.31% respectively with an excess energy of 6689.38 kWh (6.05%). It shows that the optimal configuration of the IRES at 10% DL is economically oversized by 8.31% with respect to the DL free optimal system. The results demonstrate that the overall economic value of the IRES is substantially increased with the rise in distribution losses.

7.3. *Comparison of simulation results*

The simulation results as discussed in Section 7.1 and 7.2 are compared for the optimal IRES configuration based on the various parameters and given in Table 11.

8. Sensitivity Analysis

The sensitivity analysis is performed for the off-grid IRES to predict the system behavior with the variation in

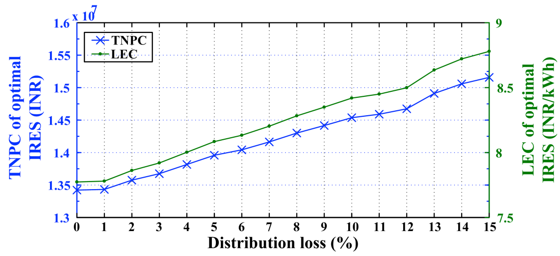

Fig. 13. TNPC and LEC of optimal IRES at different DL value

Table 11. Comparison of simulation results with and without DL

Sr. No.	Parameter	Unit	Optimal IRES without considering DL	Optimal IRES with 10 % DL	Variation observed
1	TNPC	INR	13421752.84	14537289.65	1115536.81
2	LEC	INR/kWh	7.77	8.42	0.65
3	EIR	%	94.27 @10% DL	---	---
3	SPV module	Nos.	53	73	20
4	WTG	Nos.	2	3	1
5	Battery	Nos.	45	53	8
6	EE generated	kWh	5246.26	6689.38	1443.12
7	EOSF	%	---	8.31 w.r.t DL free optimal IRES	---

influencing parameters. The sensitivity analysis has been performed to examine the economic behavior of the IRES with the variation in raw fuel (agro-forest biomass and cattle dung) cost and the capital cost of the system components. The DL of 10% has been considered in the analysis and the optimal IRES configuration is obtained for each input.

8.1. Increment in biomass cost

In order to consider the variation in cost of biomass, the biomass cost increment factor is introduced in the simulation. The value of the biomass cost increment factor has been considered from 5% to 50% in the step of 5%. At each value of the biomass cost increment factor, the optimal configuration of the IRES with 10% DL has been evaluated. The TNPC and LEC of the optimal system at each value of the biomass cost increment factor are shown in Fig. 15. These results show that the TNPC of the optimal IRES varies from INR 14573528.05 to INR 15717620.62 for the biomass cost increment factor of 5% to 50% respectively. Further, the corresponding LEC varies from 8.44 INR/kWh to 9.10 INR/kWh.

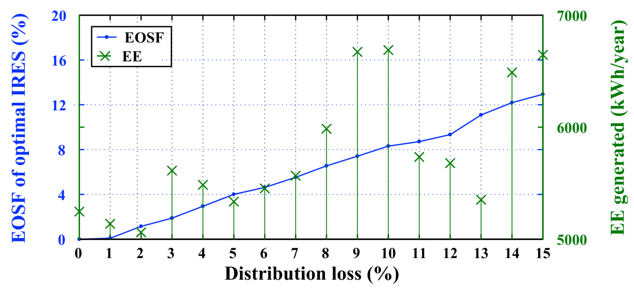

Fig. 14. EOSF with EE at different DL value

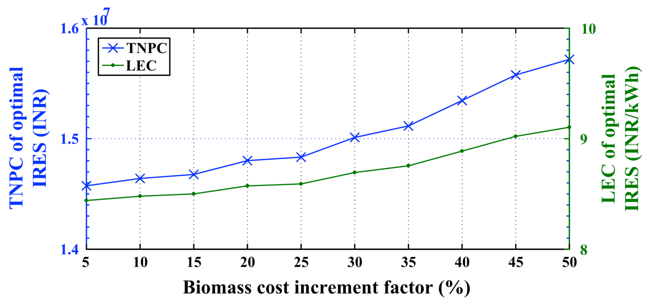

Fig. 15. Effect of biomass cost on TNPC and LEC

8.2. Increment in cattle dung cost

The cost increment factor has been introduced in the simulation to consider the variation in cattle dung cost. The value of the cost increment factor has been varied from 5% to 50% in the step of 5%, and the simulation results are obtained. At each value of the cost increment factor, the optimal configuration of IRES is obtained and corresponding TNPC and LEC are evaluated. The TNPC and LEC of the optimal IRES at each cost increment factor are shown in Fig. 16. These results show that the TNPC of the optimal IRES varies from INR 14601208.69 to INR 15013119.72 for the cost increment factor of 5% to 50% respectively. Further, the corresponding LEC varies from 8.46 INR/kWh to 8.70 INR/kWh. From Fig. 15 and Fig. 16, it has been observed that the proposed IRES model is more sensitive to the variation in cost of biomass compared to the cost of cattle dung.

8.3. Variation in capital cost of IRES components

The capital cost variation factor, from -20% to +20 % in the step of 5%, is used in the simulation to vary the capital cost of the IRES components, and the optimal TNPC of the IRES are evaluated. The variation in TNPC of the optimal IRES with variation in capital cost of the different components is shown in Fig. 17. At 20% increment in the capital cost of SPV, WTG, BMG, BGG, battery and BDC-CC, the corresponding TNPC of the optimal IRES are observed as INR 14695413.51, INR 14701089.65, INR 14936167.90, INR 14691459.89, INR 14941155.60 and INR 14626200.02 respectively. Also, at 20% decrement in the capital cost of SPV, WTG, BMG, BGG, battery and BDC-CC, the corresponding TNPC of the optimal IRES are

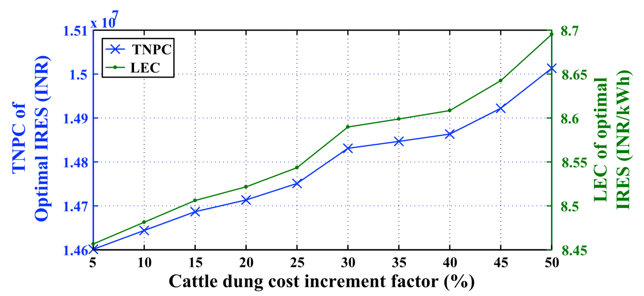

Fig. 16. Effect of cattle dung cost on TNPC and LEC

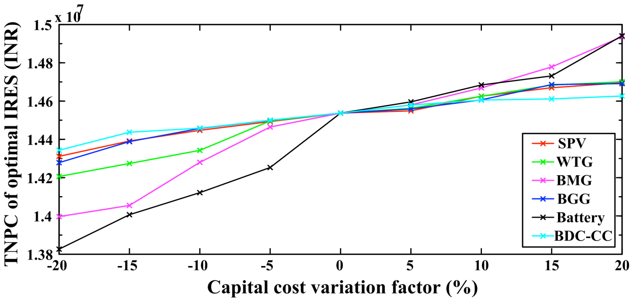

Fig. 17. Effect of variation in capital cost of IRES component on TNPC

observed as INR 14311065.64, INR 14205923.93, INR 13996311.80, INR 14278231.87, INR 13826539.58 and INR 14343491.74 respectively. From Fig. 17, it is seen that the TNPC of the optimal IRES is significantly changed with the variation in capital cost of the different IRES components. These results show that the proposed IRES model is more sensitive to the variation in capital cost of the battery and BMG compared to other system components.

9. Break-even Analysis for Grid Extension Distance

The break-even analysis for the grid extension distance determines how far the off-grid site should be from an existing distribution point so that the off-grid system is cost effective compared to constructing the transmission line [72]. In order to identify the break-even point, the TNPC of grid extension has been evaluated and compared with the TNPC of the optimal IRES. The TNPC of grid extension has been evaluated by considering the capital cost of the transmission line, cost of tapping from the last distribution point, O&M cost of the line and energy consumption cost. The capital costs of the transmission line and tapping from the last distribution point are taken as INR 875431/km and INR 5918 respectively. The O&M cost and aggregate energy consumption charge have been taken as 2.5% of the capital cost of transmission line and 4 INR/kWh respectively. The above mentioned cost data were obtained from the administrative office of the UGVCL, Mehsana, Gujarat, India for FY 2016-17. The TNPC of the grid along with the TNPC of the DL free IRES and IRES with 10% DL are plotted against the length of transmission line as shown in Fig. 18. From Fig. 18, it has been observed that the break-even points for the DL free optimal IRES and optimal IRES with 10% DL are 4.762 km and 5.674 km respectively. These results show that the break-even point is affected by the DL. At 10% DL, the break-even distance of the optimal IRES is increased by 0.912 km than DL free optimal system. However, the break-even distance in both the cases are less than 8 km, hence the proposed IRES can provide more cost effective means for rural electrification in the study area than grid extension. Moreover, it is also observed that the TNPC of grid extension after break-even points is considerably increased and reaches to INR 17383022.68 at 8 km line length. Thus, the proposed IRES model is found a feasible option for rural electrification in the study area against grid extension provided its TNPC is below INR 17383022.68.

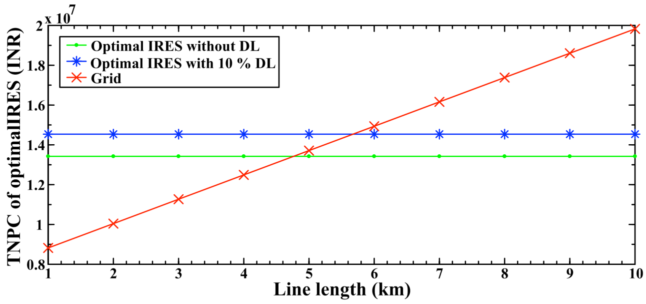

Fig. 18. Break-even analysis for grid extension distance

10. Conclusions

In this study, the modeling and economic analysis of the off-grid IRES for electrification of the remote rural area having scattered population has been undertaken. The IRES model is developed using locally available renewable energy sources such as solar, wind, biomass and biogas, and optimized by using the PSO algorithm in MATLAB environment. The results were validated by using GA. Further, an impact of the distribution losses on the power reliability, component size and economy of the IRES has been demonstrated. It has been found that the distribution losses significantly affect the power reliability, if not considered during IRES design. Furthermore, the results demonstrated that the system component size and overall economy of the IRES are considerably increased with the rise in distribution losses. The results also indicate that the proposed IRES model is more sensitive for the variation in biomass cost and capital cost of the battery and BMG. Further analysis showed that the proposed integrated system is economically feasible option for rural electrification of the considered study area rather than grid extension. The proposed IRES model can be useful for prediction of the impact of distribution losses on the power reliability, economy and size of the IRES before actual implementation. Moreover, the economic viability of the project can be predicted for any size and configuration of the IRES, which can be useful in planning and policy-making of the off-grid IRES based projects having scattered loads.

Acknowledgement

The authors gratefully acknowledge the research facilities provided by the Quality Improvement Program (QIP) centre and Alternate Hydro Energy Centre (AHEC), IIT Roorkee, India. The authors also wish to express gratitude to All India Council for Technical Education (AICTE), India for providing financial assistance in the form of research scholarship. Sincere thanks are also given to Commissioner of Technical Education, Gujarat state, India and Government Engineering College, Palanpur, Gujarat state, India for providing financial support to conduct this study. We gratefully acknowledge the meteorological data provided by the Indian Meteorological Department (IMD), Pune, India.

Abbreviations

BDC-CC	Bi-directional converter with charge controller	LEC	Levelized energy cost
BGG	Biogas generator	LED	Light emitting diode
BMG	Biomass generator	O&M	Operation and maintenance
DL	Distribution losses	PSO	Particle swarm optimization
EE	Excess energy	PV	Photovoltaic
EENS	Expected energy not supplied	RE	Renewable energy
EIR	Energy index of reliability	RES	Renewable energy sources
EOSF	Economic oversize factor	SOC	State of charge
GA	Genetic algorithm	SPV	Solar photovoltaic
GEDA	Gujarat energy development agency	TNPC	Total net present cost
IMD	Indian meteorological department	UGVCL	Uttar Gujarat vij company limited
IRES	Integrated renewable energy system	WTG	Wind turbine generator

References

[1] Teegala SK, Singal SK. Optimal costing of overhead power transmission lines using genetic algorithms. Int J Electr Power Energy Syst 2016;83:298–308. doi:10.1016/j.ijepes.2016.04.031.

[2] Dekker J, Nthontho M, Chowdhury S, Chowdhury SP. Economic analysis of PV/diesel hybrid power systems in different climatic zones of South Africa. Int J Electr Power Energy Syst 2012;40:104–12. doi:10.1016/j.ijepes.2012.02.010.

[3] Intergovernmental Panel for Climate Change [IPCC]. Climate Change 2014: Synthesis Report. Geneva, Switzerland: 2014.

[4] Das HS, Dey A, Wei TC, Yatim AHM. Feasibility analysis of standalone PV/wind/battery hybrid energy system for rural Bangladesh. Int J Renew Energy Res 2016;6:402–12.

[5] Rajbongshi R, Borgohain D, Mahapatra S. Optimization of PV-biomass-diesel and grid base hybrid energy systems for rural electrification by using HOMER. Energy 2017;126:461–74. doi:10.1016/j.energy.2017.03.056.

[6] Patel AM, Singal SK. Off grid rural electrification using integrated renewable energy system. 2016 IEEE 7th Power India Int. Conf., Bikaner, Rajasthan, India: 2016, p. 1–5. doi:10.1109/POWERI.2016.8077272.

[7] Chauhan A, Saini RP. Renewable energy based off-grid rural electrification in Uttarakhand state of India: Technology options, modelling method, barriers and recommendations. Renew Sustain Energy Rev 2015;51:662–81. doi:10.1016/j.rser.2015.06.043.

[8] Guler O, Akdag SA, Cakir YS. Effects of data resolution on stand-alone hybrid system sizing. 3rd Int. Conf. Renew. Energy Res. Appl., Madrid, Spain: 2013, p. 423–7. doi:10.1109/ICRERA.2013.6749792.

[9] Cano A, Jurado F, Sánchez H, Fernández LM, Castañeda M. Optimal sizing of stand-alone hybrid systems based on PV/WT/FC by using several methodologies. J Energy Inst 2014;87:330–40. doi:10.1016/j.joei.2014.03.028.

[10] Tummuru NR, Mishra MK, Srinivas S. Dynamic Energy Management of Renewable Grid Integrated Hybrid Energy Storage System. IEEE Trans Ind Electron 2015;62:7728–37. doi:10.1109/TIE.2015.2455063.

[11] Rajini V, Amutha WM. Real time implementation of a single stage converter based Solar-Wind hybrid system. 6th Int. Conf. Renew. Energy Res. Appl., San Diego, USA: 2017, p. 1051–7. doi:10.1109/ICRERA.2017.8191218.

[12] Paragond LS, Kurian CP, Singh BK. Design and simulation of solar and wind energy conversion system in isolated mode of operation. 4th Int. Conf. Renew. Energy Res. Appl., Palermo, Italy: 2015, p. 999–1004. doi:10.1109/ICRERA.2015.7418560.

[13] Patel AM, Singal SK. Design approach of integrated renewable energy system for small autonomous power system. 2016 IEEE 7th Power India Int. Conf., Bikaner, Rajasthan, India: 2016, p. 1–5. doi:10.1109/POWERI.2016.8077266.

[14] Iqbal M, Azam M, Naeem M, Khwaja AS, Anpalagan A. Optimization classification, algorithms and tools for renewable energy: A review. Renew Sustain Energy Rev 2014;39:640–54. doi:10.1016/j.rser.2014.07.120.

[15] Mercado KD, Jiménez J, M CGQ. Hybrid renewable energy system based on intelligent optimization techniques. 5th Int. Conf. Renew. Energy Res. Appl., Birmingham, UK: 2016, p. 661–6. doi:10.1109/ICRERA.2016.7884417.

[16] Kaabeche A, Belhamel M, Ibtiouen R. Sizing optimization of grid-independent hybrid photovoltaic/wind power generation system. Energy 2011;36:1214–22. doi:10.1016/j.energy.2010.11.024.

[17] GURSOY G, BAYSAL M. Improved optimal sizing of hybrid PV/Wind/Battery energy systems. 3rd Int. Conf. Renew. Energy Res. Appl., Milwaukee, USA: 2014, p. 713–6. doi:10.1109/ICRERA.2014.7016478.

[18] Mostofi F, Shayeghi H. Feasibility and optimal reliable design of renewable hybrid energy system for rural electrification in Iran. Int J Renew Energy

Res 2012;2.

[19] Dhass AD, Harikrishnan S. Cost effective hybrid energy system employing solar-wind-biomass resources for rural electrification. Int J Renew Energy Res 2013;3:222–9.

[20] Hashim H, Ho WS, Lim JS, Macchietto S. Integrated biomass and solar town: Incorporation of load shifting and energy storage. Energy 2014;75:31–9. doi:10.1016/j.energy.2014.04.086.

[21] Rahman M, Mahmodul M, Paatero J V. Hybrid application of biogas and solar resources to fulfill household energy needs: A potentially viable option in rural areas of developing countries. Renew Energy 2014;68:35–45. doi:10.1016/j.renene.2014.01.030.

[22] Sigarchian SG, Paleta R, Malmquist A, Pina A. Feasibility study of using a biogas engine as backup in a decentralized hybrid (PV/wind/battery) power generation system - Case study Kenya. Energy 2015;90:1830–41. doi:10.1016/j.energy.2015.07.008.

[23] Barzola J, Espinoza M, Cabrera F. Analysis of hybrid solar/wind/diesel renewable energy system for off-grid rural electrification. Int J Renew Energy Res 2016;6:1146–52.

[24] Girma Z. Technical and economic assessment of solar PV/diesel hybrid power system for rural school electrification in Ethiopia. Int J Renew Energy Res 2013;3. doi:10.1080/14786451.2015.1017498.

[25] Kumar Nandi S, Ranjan Ghosh H. Techno-economical analysis of off-grid hybrid systems at Kutubdia Island, Bangladesh. Energy Policy 2010;38:976–80. doi:10.1016/j.enpol.2009.10.049.

[26] Rajanna S, Saini RP. Modeling of integrated renewable energy system for electrification of a remote area in India. Renew Energy 2016;90:175–87. doi:10.1016/j.renene.2015.12.067.

[27] Xu Z, Nthontho M, Chowdhury S. Rural electrification implementation strategies through microgrid approach in South African context. Int J Electr Power Energy Syst 2016;82:452–65. doi:10.1016/j.ijepes.2016.03.037.

[28] Upadhyay S, Sharma MP. Development of hybrid energy system with cycle charging strategy using particle swarm optimization for a remote area in India. Renew Energy 2015;77:586–98. doi:10.1016/j.renene.2014.12.051.

[29] Ismail MS, Moghavvemi M, Mahlia TMI. Genetic algorithm based optimization on modeling and design of hybrid renewable energy systems. Energy Convers Manag 2014;85:120–30. doi:10.1016/j.enconman.2014.05.064.

[30] Kanase-Patil AB, Saini RP, Sharma MP. Development of IREOM model based on seasonally varying load profile for hilly remote areas of Uttarakhand state in India. Energy 2011;36:5690–702. doi:10.1016/j.energy.2011.06.057.

[31] Mandelli S, Barbieri J, Mereu R, Colombo E. Off-grid systems for rural electrification in developing countries: Definitions, classification and a comprehensive literature review. Renew Sustain Energy Rev 2016;58:1621–46. doi:10.1016/j.rser.2015.12.338.

[32] Sultana B, Mustafa MW, Sultana U, Bhatti AR. Review on reliability improvement and power loss reduction in distribution system via network reconfiguration. Renew Sustain Energy Rev 2016;66:297–310. doi:10.1016/j.rser.2016.08.011.

[33] Jordehi AR. Optimisation of electric distribution systems: A review. Renew Sustain Energy Rev 2015;51:1088–100. doi:10.1016/j.rser.2015.07.004.

[34] Kalambe S, Agnihotri G. Loss minimization techniques used in distribution network: Bibliographical survey. Renew Sustain Energy Rev 2014;29:184–200. doi:10.1016/j.rser.2013.08.075.

[35] Viegas JL, Vieira SM, Esteves PR, Melício R, Mendes VMF. Solutions for detection of non-technical losses in the electricity grid: a review. Renew Sustain Energy Rev 2017;80:1256–68. doi:10.1016/j.rser.2017.05.193.

[36] Sultana U, Khairuddin AB, Aman MM, Mokhtar AS, Zareen N. A review of optimum DG placement based on minimization of power losses and voltage stability enhancement of distribution system. Renew Sustain Energy Rev 2016;63:363–78. doi:10.1016/j.rser.2016.05.056.

[37] GoI. Maps of protected areas in India. ENVIS Cent Wildl Prot Area 2011. http://wiienvis.nic.in/Database/Maps_PAs_1267.aspx (accessed November 29, 2016).

[38] WRISI. Map of Gujarat 2015. http://www.india-wris.nrsc.gov.in/wrpinfo/index.php?title=Gujarat (accessed November 29, 2016).

[39] GoG. Forest GIS map 2016. https://forests.gujarat.gov.in/forest-gis-map.htm (accessed November 29, 2016).

[40] Google. Google Earth 2016. https://www.google.com/earth/ (accessed November 29, 2016).

[41] Diouf B, Pode R, Osei R. Initiative for 100% rural electrification in developing countries: Case study of Senegal. Energy Policy 2013;59:926–30. doi:10.1016/j.enpol.2013.04.012 Communication.

[42] GEDA. Gujarat: The renewable energy potential. Gujarat Informatics Ltd 2017. https://geda.gujarat.gov.in/background.php (accessed March 28, 2017).

[43] Murthy KSR, Rahi OP. Preliminary assessment of wind power potential over the coastal region of Bheemunipatnam in northern Andhra Pradesh, India. Renew Energy 2016;99:1137–45. doi:10.1016/j.renene.2016.08.017.

[44] Patel MR. Wind and solar power systems: Design, Analysis, and Operation. 2nd ed. Boca Raton: CRC Press; 2006.

[45] GoG. District statistics n.d. https://banaskanthadp.gujarat.gov.in/banaskantha/prkashano/prakasano.htm (accessed October 14, 2016).

[46] GEDA. Manufacturer list. Gujarat Informatics Ltd 2017. https://geda.gujarat.gov.in/system_manufacturer_list.php (accessed March 28, 2017).

[47] MNRE. List of manufacturer empanelled 2016. http://mnre.gov.in/information/manufacturesindustrie

sarchitectsconsulting-organisation/ (accessed December 18, 2016).
[48] Chauhan A, Saini RP. Discrete harmony search based size optimization of integrated renewable energy system for remote rural areas of Uttarakhand state in India. Renew Energy 2016;94:587–604. doi:10.1016/j.renene.2016.03.079.
[49] Chauhan A, Saini RP. Size optimization and demand response of a stand-alone integrated renewable energy system. Energy 2017;124:59–73. doi:10.1016/j.energy.2017.02.049.
[50] Chauhan A. Evolving optimal integrated renewable energy system model for stand-alone applications. Indian Institute of Technology, Roorkee, 2015.
[51] Mondal AH, Denich M. Hybrid systems for decentralized power generation in Bangladesh. Energy Sustain Dev 2010;14:48–55. doi:10.1016/j.esd.2010.01.001.
[52] Gupta RA, Kumar R, Bansal AK. BBO-based small autonomous hybrid power system optimization incorporating wind speed and solar radiation forecasting. Renew Sustain Energy Rev 2015;41:1366–75. doi:10.1016/j.rser.2014.09.017.
[53] Rajanna S, Saini RP. Development of optimal integrated renewable energy model with battery storage for a remote Indian area. Energy 2016;111:803–17. doi:10.1016/j.energy.2016.06.005.
[54] McKendry P. Energy production from biomass (part 1): overview of biomass. Biosource Technol 2002;83:37–46. doi:10.1016/S0960-8524(01)00118-3.
[55] Singh J, Panesar BS, Sharma SK. Energy potential through agricultural biomass using geographical information system-A case study of Punjab. Biomass and Bioenergy 2008;32:301–7. doi:10.1016/j.biombioe.2007.10.003.
[56] Gupta A, Saini RP, Sharma MP. Steady-state modelling of hybrid energy system for off grid electrification of cluster of villages. Renew Energy 2010;35:520–35. doi:10.1016/j.renene.2009.06.014.
[57] Goodbody C, Walsh E, McDonnell KP, Owende P. Regional integration of renewable energy systems in Ireland – The role of hybrid energy systems for small communities. Int J Electr Power Energy Syst 2013;44:713–20. doi:10.1016/j.ijepes.2012.08.012.
[58] Agarwal N, Kumar A, Varun. Optimization of grid independent hybrid PV-diesel-battery system for power generation in remote villages of Uttar Pradesh, India. Energy Sustain Dev 2013;17:210–9. doi:10.1016/j.esd.2013.02.002.
[59] Askarzadeh A. Developing a discrete harmony search algorithm for size optimization of wind-photovoltaic hybrid energy system. Sol Energy 2013;98:190–5. doi:10.1016/j.solener.2013.10.008.
[60] Mukhtaruddin RNSR, Rahman HA, Hassan MY, Jamian JJ. Optimal hybrid renewable energy design in autonomous system using Iterative-Pareto-Fuzzy technique. Int J Electr Power Energy Syst 2015;64:242–9. doi:10.1016/j.ijepes.2014.07.030.
[61] Kanase-Patil AB, Saini RP, Sharma MP. Sizing of integrated renewable energy system based on load profiles and reliability index for the state of Uttarakhand in India. Renew Energy 2011;36:2809–21. doi:10.1016/j.renene.2011.04.022.
[62] GERC. Tariff order for UGVCL. Tarif Orders n.d. http://www.gercin.org/orders.aspx?o_cat=1 (accessed April 2, 2017).
[63] Tina G, Gagliano S, Raiti S. Hybrid solar/wind power system probabilistic modelling for long-term performance assessment. Sol Energy 2006;80:578–88. doi:10.1016/j.solener.2005.03.013.
[64] Askarzadeh A, dos Santos Coelho L. A novel framework for optimization of a grid independent hybrid renewable energy system: A case study of Iran. Sol Energy 2015;112:383–96. doi:10.1016/j.solener.2014.12.013.
[65] Kennedy J, Eberhart R. Particle Swarm Optimization. IEEE Int. Conf. neural networks, Perth, WA, Australia: 1995, p. 1942–8. doi:10.1109/ICNN.1995.488968.
[66] Moradi MH, Eskandari M, Showkati H. A hybrid method for simultaneous optimization of DG capacity and operational strategy in microgrids utilizing renewable energy resources. Int J Electr Power Energy Syst 2014;56:241–58. doi:10.1016/j.ijepes.2013.11.012.
[67] Arabali A, Ghofrani M, Etezadi-Amoli M, Fadali MS, Baghzouz Y. Genetic-algorithm-based optimization approach for energy management. IEEE Trans Power Deliv 2013;28:162–70. doi:10.1109/TPWRD.2012.2219598.
[68] Katsigiannis YA, Georgilakis PS, Karapidakis ES. Genetic Algorithm Solution to Optimal Sizing Problem of Small Autonomous Hybrid Power Systems. Artificaial Intell. Theor. Model. Appl., 2010, p. 327–32. doi:10.1007/978-3-642-12842-4_38.
[69] Koutroulis E, Kolokotsa D, Potirakis A, Kalaitzakis K. Methodology for optimal sizing of stand-alone photovoltaic/wind-generator systems using genetic algorithms. Sol Energy 2006;80:1072–88. doi:10.1016/j.solener.2005.11.002.
[70] Katsigiannis YA, Georgilakis PS, Karapidakis ES. Multiobjective genetic algorithm solution to the optimum economic and environmental performance problem of small autonomous hybrid power systems with renewables. IET Renew Power Gener 2010;4:404–19. doi:10.1049/iet-rpg.2009.0076.
[71] RBI. RBI Bulletin: September 2016. vol. 30. 2016.
[72] Mahapatra S, Dasappa S. Rural electrification: Optimising the choice between decentralised renewable energy sources and grid extension. Energy Sustain Dev 2012;16:146–54. doi:10.1016/j.esd.2012.01.006.